J. CHEM. SOC. FARADAY TRANS., 1992, 88(12), 1643–1651

Rotational Brownian Motion of the Proton Crane operating in a Photoinduced Long-distance Intramolecular Proton Transfer

C. Jojakim Jalink, A. Herbert Huizer and Cyril A. G. O. Varma*
State University Leiden, Chemistry Department, Gorlaeus Laboratories, P.O. Box 9502, 2300 RA Leiden, The Netherlands

The photoinduced proton transfer from the OH group to the endocyclic N atom in 7-hydroxy-8-(*N*-morpholinomethyl)quinoline (HMMQ) has been studied as a function of temperature at constant viscosity and as a function of viscosity at constant temperature for solutions in alkanols and in alkanenitriles. The overall rate constant, k, is determined by the rotational motion of the side group. There is an energy barrier on the reaction path, which does not depend on the solvent. The motion along the reaction path is described as the Brownian motion of a particle suffering hydrodynamic friction and moving under the influence of an intramolecular Coulomb potential and disappearing at a sink. The influence of dielectric friction is neglected. The friction coefficient is considered to be time-independent. The resulting Smoluchowski equation is solved numerically, using initial and boundary conditions imposed by intramolecular hydrogen bonds required for proton transfer. A good agreement between theory and experiment is obtained. A fractional power dependence of k on viscosity is obtained, which is not the same for alkanols and nitriles as solvents. This difference is attributed to a back transfer of the proton to its original site in the case of nitriles. In the case of alkanols, the back transfer is blocked by hydrogen bonding of the original site with the solvent, after the initial deprotonation of the OH group.

In several branches of chemistry there is a great deal of interest in a knowledge of the factors which influence the motion of flexible molecular chains or of nearly free rotors. A prerequisite in a precise study of such motions is that the molecular conformations are known at the beginning and at the end of the trajectory. Recently we have drawn attention to the possibility of using a photoinduced intramolecular proton-transfer reaction to study the dynamics of a flexible alkyl chain.[1,2] Since a proton-transfer process is restricted to an extremely narrow range of distances between donor and acceptor sites, it is conceivable to take advantage of proton transfer as a means of defining the initial and final conformations. This might be achieved, when *e.g.* one end of a flexible chain carries a donor, while the acceptor is localized on the other end. Then the proton-transfer process is possible only in those conformations in which the end-to-end distance is comparable to a hydrogen-bonding distance. We have reported on a multistep intramolecular proton-transfer process in which such a situation is encountered twice. The report concerns the photoinduced transfer of a proton from the hydroxyl group to the N atom in the quinoline ring in 7-hydroxy-8-(*N*-morpholinomethyl)quinoline (HMMQ, Fig. 1).[2] In the electronic ground state, HMMQ exists only in the enol form (E), which has an intramolecular hydrogen bond between the hydroxyl group and the nitrogen atom N(2) in the morpholino ring. In the first excited singlet electronic state (E*) the acidity of the hydroxy proton is enhanced relative to the ground state. Upon electronic excitation the proton is initially transferred adiabatically from the hydroxyl to the morpholino group, resulting in the zwitterionic tautomer (A*) of HMMQ. This first step was found to be very fast ($k_{PT} > 2 \times 10^{11}$ s^{-1}) and in accordance with the existence of a hydrogen bond prior to excitation. Since the excitation causes also a large increase in the proton affinity of the nitrogen atom N(1) in the quinoline ring, it may accept the proton residing on the morpholino ring, when this comes within hydrogen-bonding distance. The protonation of N(1) proceeds adiabatically and yields the electronically excited keto tautomer (K*) of HMMQ. Of course, the protonation of N(1) is feasible only after completion of the rotation of the side group over 180°, as required to establish a hydrogen bond between protonated N(2) and N(1). This new hydrogen bond defines the final state of the rotational motion, whereas the initial state is defined by the hydrogen bond in E. Both the first (*i.e.* E* → A*) and last (A* → K*) proton-transfer steps are accompanied by significant changes in the fluorescence spectrum of the excited sample. A study of the time dependence of these spectral changes provides information concerning the dynamics involved during the rotation.

The efficiency of the intramolecular photoreaction of HMMQ just described depends on both the rate constant k_{rot}, for the transition from the initial to final conformation of the side group, and the rate constant k_d for the decay of the excited molecule along all its other available pathways. Only when k_{rot} is comparable to or larger than k_d does one observe the double proton-transfer reaction. Therefore, chain dynamics may be studied, in photoexcited systems like HMMQ, up to a time limit of $1/k_d$. The photoreaction of HMMQ is in this regime and solvent polarity as well as solvent viscosity were shown to play a vital role in the excited state dynamics.[2] In this paper we will discuss the influence of

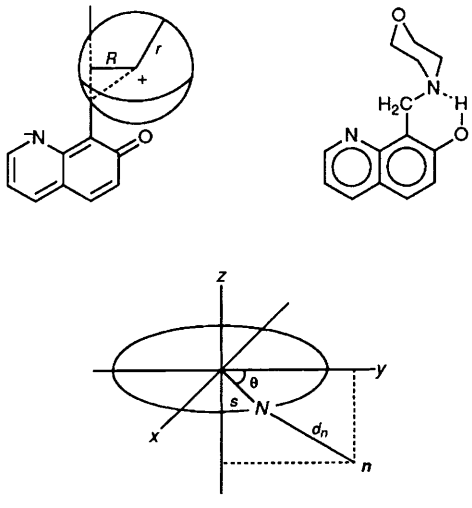

Fig. 1 Structural formula of 7-hydroxy-8-(*N*-morpholinomethyl) quinoline (HMMQ). Also shown is the coordinate system, the rotational coordinate θ, the hydrodynamic radius r of the morpholino group, and the radius of gyration R

these latter factors on the magnitude of k_{rot}. Since in the overall tautomerization of HMMQ the rotation of the side chain is the rate-limiting process, we will consider here the motion of A* along the coordinate θ (see Fig. 1). We will refer to the number of molecules of type A* as the population A* and will denote this number by N_{A^*}. The side chain rotation in the excited-state reaction of HMMQ is modelled as a damped motion of a Brownian particle on a potential surface. In this purely classical description, we will follow the treatment of the dynamics of activationless reactions, given by Bagchi *et al.*[3] In our model a position-dependent sink is used to represent the actual loss of the proton on N(2) at the site of N(1), while a position-independent sink is used to mimic the decay of the population A* along all other pathways. As a consequence of the presence of the position-dependent sink, the time dependence of the population A* has a dependence on the motion of the Brownian particle over the potential surface. This motion is driven by a random force, due to the thermal motion of solvent molecules and is further influenced by both the inertial force arising from the potential and the viscous drag due to friction with the solvent.

At first we will present the formal aspects of the theory and then we will describe the numerical procedure for finding the time dependence of the probability distribution for the population A*. Subsequently, we will discuss the numerical values of the parameters needed in the calculation of this distribution. Finally, the results of the numerical calculation will be compared with experimental results.

Equation of Motion

The probability density of finding the excited anion (A*) with the side chain in an interval between θ and $\theta + d\theta$ at a time between t and $t + dt$ will be represented by $P(\theta, t)$. A Fokker–Planck type equation of motion for $P(\theta, t)$ is the starting point of our theoretical description:[4–6]

$$\frac{\partial P(\theta, t)}{\partial t} = LP(\theta, t) - k_{PT} S(\theta) P(\theta, t) - k_d P(\theta, t) \qquad (1)$$

The rotation coordinate θ is defined in such a way, see Fig. 1, that $\theta = 0$ corresponds to the initial side-chain conformation when an H bond exists between the hydroxy group and the morpholino group. The final conformation in which an H bond is formed between the protonated aliphatic nitrogen and the quinoline nitrogen then corresponds to $\theta = \pi$. The position-dependent sink function is represented by $S(\theta)$ and assumes non-zero values in the neighbourhood of $\theta = \pi$ only. k_{PT} is a measure of the A* → K* proton-transfer rate constant from the sink, while k_d represents the position-independent (non)-radiative decay rate constant. For overdamped motion of the Brownian particle along the excited-state potential surface the operator L is given by the Smoluchowski operator

$$L_S = D\left(\frac{\partial^2}{\partial\theta^2} - \frac{1}{k_B T}\frac{\partial}{\partial\theta} F(\theta)\right) \qquad (2)$$

where $D = k_B T/\xi$ is the diffusion coefficient and ξ is the relevant friction coefficient. The force on the Brownian particle is given by $F = -\partial V/\partial\theta$, where $V(\theta)$ is the excited-state potential. The term LP in eqn. (1) describes the motion of the Brownian particle over the potential surface, while $[k_{PT} S(\theta) + k_d]P$ represents the rate of loss of the population A* due to the proton-transfer process and electronic relaxation. Such an equation has been used by Bagchi *et al.*[3,7] in the treatment of the dynamics of activationless reactions in solutions and also by Marcus and co-workers[8,9] in the theoretical study of solvent effects on non-adiabatic electron-transfer reactions.

The initial, boundary and symmetry conditions for $P(\theta, t)$ with which we solve eqn. (1) are given by

$$P(\theta, t = 0) = \left(\frac{I\omega^2}{2\pi k_B T}\right)^{1/2} \exp\left(-\frac{I\omega^2\theta^2}{2k_B T}\right)$$
$$P(\theta = \pm\pi, t) = 0 \qquad (3)$$
$$P(\theta, t) = P(-\theta, t)$$

The first of these relations expresses the fact that $P(\theta, t)$ is normalized to 1 at $t = 0$. The quantity I represents the moment of inertia of the morpholino group with respect to the rotation axis. ω is the frequency of the torsional vibration of this group around $\theta = 0$. Note that the boundary condition at $\theta = \pm\pi$ depends on the analytical form of the sink function $S(\theta)$ and on the magnitude of the proton-transfer rate constant k_{PT}. The boundary condition given in the second relation is valid only if $k_{PT} = \infty$, while the sink function is represented by a Dirac delta function, *i.e.* if $S(\theta) = \delta(\theta \pm \pi)$. This case corresponds to the infinite pinhole sink discussed by Bagchi *et al.* When k_{PT} is finite or when $S(\theta)$ is not given by a Dirac delta function but by *e.g.* a Gaussian function, this boundary condition is inappropriate, because then $P(\theta, t)$ can assume any finite value at $\theta = \pi$. The third relation imposes a symmetry condition, originating from the definition of the coordinate θ.

From the steady-state and time-resolved fluorescence experiments reported previously it has been concluded that the various conformations of A* are indistinguishable.[2] This fact is taken into account by introducing the probability $P_e(t)$ of finding the Brownian particle still in the excited state at time t, regardless of the conformational coordinate θ. This probability is given by

$$P_e(t) = \int_{-\pi}^{\pi} d\theta P(\theta, t) \qquad (4)$$

If we set $N_{A^*} = 1$ at $t = 0$, $P_e(t)$ may be considered to represent the population A* at time t, *i.e.* $P_e(t) = N_{A^*}(t)$. It is the time dependence of $N_{A^*}(t)$ which is monitored in the time-resolved fluorescence experiments. The time-averaged decay rate k of $N_{A^*}(t)$ is now given by

$$k^{-1} = \int_0^{\infty} dt P_e(t) \qquad (5)$$

Choice of Basis Functions

We have not been successful in finding an analytical solution for $P(\theta, t)$. Therefore we approached this problem numerically by expanding $P(\theta, t)$ into a set of orthonormal basis functions $\{B_n(\theta)\}$. The solution is then given by

$$P(\theta, t) = \sum_{n=0}^{\infty} p_n(t) B_n(\theta) \qquad (6)$$

Using this expansion, eqn. (1) may be converted into a set of linear equations in the expansion coefficient $p_n(t)$. These can be written in the form of the matrix equation

$$\dot{\boldsymbol{p}}(t) = \boldsymbol{M} \cdot \boldsymbol{p}(t) \qquad (7)$$

in which the matrix elements $M_{m,n}$ are real and are given by

$$M_{m,n} = \langle B_m(\theta) | L_S(\theta) - k_{PT} S(\theta) - k_d | B_n(\theta) \rangle \qquad (8)$$

The brackets in eqn. (8) indicate integration over θ from $-\pi$ to π. The formal solution of eqn. (7) may be written as

$$\boldsymbol{p}(t) = \exp(\boldsymbol{M}t) \cdot \boldsymbol{p}(0) \qquad (9)$$

where $\boldsymbol{p}(0)$ is obtained from $P(\theta, 0)$ given in eqn. (3).

Referring to Fig. 1 for the definition of the rotation coordinate θ, it is clear from symmetry considerations that the intramolecular potential $V(\theta)$ may be expanded in the set $\{\cos n\theta\}$ as the Fourier series

$$V(\theta) = \sum_{n=0}^{\infty} v_n \cos n\theta \tag{10}$$

Note that the most appropriate choice of the basis set $\{B_n(\theta)\}$ depends on the analytical form of the sink function $S(\theta)$. When $S(\theta)$ is a Gaussian function, the most convenient choice is $B_n(\theta) = \cos n\theta$. However, if $S(\theta)$ is a delta function, the expansion of $P(\theta, t)$ in the set $\{\cos n\theta\}$ results in a very awkward matrix $\boldsymbol{M}$, which leads to numerical problems to be discussed later on. In the case of the delta function, it is preferable to expand $P(\theta, t)$ in the basis set $\{\cos(n + 1/2)\theta\}$. Both of these functional forms of $S(\theta)$ will be discussed separately.

Gaussian Sink

Consider a Gaussian sink, with an FWHM of $\sqrt{(8 \ln 2\sigma_s^2)}$, centred around $\theta = \pm\pi$. The function $S(\theta)$ is then given by

$$S(\theta) = \frac{1}{\sqrt{(2\pi\sigma_s^2)}} \exp\left(-\frac{(\theta - \pi)^2}{2\sigma_s^2}\right) \tag{11}$$

When $P(\theta, t)$ is expanded in the basis set $B_n(\theta) = \{\cos n\theta\}$, the elements of the matrix $\boldsymbol{M}$ are given by

$$M_{m,m} = -Dm^2 - \frac{\pi c_m^2}{2\xi} I_{m,m} - k_{PT} c_m^2 S_{m,m} - k_d$$

$$M_{m,n} = -\frac{\pi c_m c_n}{2\xi} I_{m,n} - k_{PT} c_m c_n S_{m,n} \tag{12}$$

where $c_n = \sqrt{(2\pi)}$ for $n = 0$ and $c_n = \sqrt{(\pi)}$ for $n \geqslant 1$, and in which $I_{m,n}$ and $S_{m,n}$ are given by

$$I_{m,n} = \sum_{l=0}^{\infty} (l + n) l v_{l+n} \delta_{l,m} - \sum_{l=0}^{n} (n - l) l v_{n-l} \delta_{l,m} + \sum_{l=n}^{\infty} (l - n) l v_{l-n} \delta_{l,m}$$

$$S_{m,n} = \frac{(-1)^{m+n}}{2} \{\exp[-(m - n)^2\sigma_s^2/2] + \exp[-(m + n)^2\sigma_s^2/2]\} \tag{13}$$

When the Gaussian sink has a finite width, *i.e.* $\sigma_s > 0$, the off-diagonal elements of $\boldsymbol{S}$ decrease exponentially as a function of the index number. The basis set may then be truncated after a value $n = n_{max}$. Note that in the limit $\sigma_s \to 0$, the Gaussian function becomes a delta function.

Using $B_n(\theta) = \{\cos n\theta\}$, the resulting expression for $P_e(t)$ is

$$P_e(t) = 2\pi p_0(t) \tag{14}$$

Since the fluorescence intensity is proportional to $P_e(t)$, its time dependence is governed, according to eqn. (14), only by the first basis function. If the width (FWHM) of the initial Gaussian distribution is equal to $\sqrt{(8 \ln 2\sigma_i^2)}$, the time-averaged decay constant of $N_{A^*}(t)$ is given by

$$k^{-1} = -2\pi \sum_{n=0}^{\infty} (M^{-1})_{0,n} p_n(0) = -2\pi \sum_{n=0}^{\infty} (M^{-1})_{0,n} c_n^2 \exp(-n^2\sigma_i^2/2) \tag{15}$$

Infinite Pinhole Sink

If the proton transfer from atom N(2) to atom N(1) takes place only within an extremely narrow range of distances between these atoms, the analytical form of the function $S(\theta)$ may be taken as a delta function. When $S(\theta) = \delta(\theta + \pi)$, the Brownian particle is lost from the population N_{A^*} with unit probability upon arriving at $\theta = \pi$. Mathematically, this model corresponds to the well known problem of Brownian motion in the presence of an absorbing barrier.[4–6] Then the boundary condition is given by the second relation in eqn. (3). In the case of the delta function sink, a convenient basis set for expanding $P(\theta, t)$ is $B_n(\theta) = \{\cos(n + 1/2)\theta\}$, because each of these functions satisfies the boundary conditions. The elements of the matrix $\boldsymbol{M}$ are then given by

$$M_{m,m} = -D\left(m + \frac{1}{2}\right)^2 - \frac{1}{2\xi} I_{m,m} - k_d$$

$$M_{m,n} = -\frac{1}{2\xi} I_{m,n} \tag{16}$$

in which $I_{m,n}$ is given by

$$I_{m,n} = \sum_{l=0}^{\infty} (l + n + 1)(l + \tfrac{1}{2}) v_{l+n+1} \delta_{l,m} - \sum_{l=0}^{n} (n - l)(l + \tfrac{1}{2}) v_{n-l} \delta_{l,m} + \sum_{l=n}^{\infty} (l - n)(l + \tfrac{1}{2}) v_{l-n} \delta_{l,m} \tag{17}$$

The second term on the right-hand side of eqn. (1) does not contribute to the matrix elements of $\boldsymbol{M}$ in eqn. (16). This is a consequence of the choice of the basis $B_n(\theta) = \{\cos(n + 1/2)\theta\}$. From eqn. (13) it may be inferred that in the limit of an infinitesimal width of the Gaussian sink, *i.e.* as $\sigma_s \to 0$, all elements of the matrix $\boldsymbol{S}$ are ± 1. This result is also obtained by using $B_n(\theta) = \{\cos n\theta\}$ and $S(\theta) = \delta(\theta \pm \pi)$. However, in the latter case unresolvable problems are encountered in the inversion of the matrix $\boldsymbol{M}$. The reason for this is the sink contribution to the off-diagonal elements of $\boldsymbol{M}$ in eqn. (12). These difficulties do not appear in the case $B_n(\theta) = \{\cos(n + 1/2)\theta\}$. The off-diagonal elements of $\boldsymbol{M}$ in eqn. (16) are then completely determined by the expansion coefficients of the intramolecular potential as given by eqn. (10) and the basis set may again be truncated after a value $n = n_{max}$.

In the basis $B_n(\theta) = \{\cos(n + 1/2)\theta\}$, the expression for the probability for finding a particle in the excited state after a time t is given by

$$P_e(t) = \sum_{n=0}^{\infty} \frac{2(-1)^n}{n + \frac{1}{2}} p_n(t) \equiv \boldsymbol{f} \cdot \boldsymbol{p}(t) \tag{18}$$

Since the fluorescence intensity is proportional to $P_e(t)$, it follows from eqn. (18) that all basis functions contribute to the time dependence of this intensity. This is in contrast with the result in eqn. (14), where only the first basis function makes a contribution.

The time-averaged relaxation rate of N_{A^*} obtained in the basis $B_n(\theta) = \{\cos(n + 1/2)\theta\}$ is given by

$$k^{-1} = -\boldsymbol{f} \cdot \boldsymbol{M}^{-1} \cdot \boldsymbol{p}(0) = -\frac{1}{\pi} \sum_{m,n=0}^{\infty} \frac{2(-1)^m}{m + \frac{1}{2}} (M^{-1})_{m,n} \exp[-(n + \tfrac{1}{2})^2\sigma_i^2/2] \tag{19}$$

Model Parameters

A number of parameters entering in the numerical evaluation of $P(\theta, t)$ are determined by experimental facts. These are the

friction coefficient ξ; the moment of inertia I of the rotating morpholino group; the frequency ω of the torsional vibration; the intramolecular potential $V(\theta)$; the rate constants k_{PT} and k_d. However, the width of the sink function cannot be derived from experiment, but has to be chosen *a priori*.

Since the Brownian particle is in fact the protonated morpholino group, we assume hydrodynamic friction with stick boundary conditions in accordance with size and charge of the particle. We consider the morpholino group as a sphere with a hydrodynamic radius r. The friction coefficient ξ is then given by

$$\xi = 6\pi\eta r R^2 \tag{20}$$

where η is the zero-frequency shear viscosity of the solvent and R represents the radius of gyration of the morpholino group with respect to the axis of rotation. The latter is defined by $I \equiv MR^2$, where M is the molar mass of the group. We set r equal to the value of the molecular radius, obtained from the molar mass M and the density ρ of liquid morpholine. This yields $r = 3.26$ Å. Using bond lengths and angles in the morpholino group, we calculate the gyration radius with respect to the rotation axis, *i.e.* the axis passing through the C(8)—CH_2 bond in HMMQ (see Fig. 1). The result is $R = 2.73$ Å. Taking $\omega = 4$ ps^{-1} for the frequency of the oscillation of the particle around $\theta = 0$ and using eqn. (3), we obtain a width of 20° FWHM for $P(\theta, 0)$.

The potential $V(\theta)$ arises from the Coulomb attraction between the two oppositely charged moieties in the zwitterion. The potential is evaluated by considering the positive charge to be fixed on atom N(2), while the negative charge is delocalized over the quinoline ring and its distribution changes continuously as a function of θ. This amounts to

$$V(\theta) = \frac{1}{4\pi\varepsilon_0} \sum_{n=1}^{11} \frac{e\rho_n(\theta)}{d_n(\theta)} = \sum_{l=0}^{\infty} v_l \cos l\theta \tag{21}$$

with $d_n(\theta)$ the distance between the positive charge e on N(2) and the negative charge $\rho_n(\theta)$ on the nth atom in the ring. In the coordinate system presented in Fig. 1, the atom N(2) moves along the circumference of a circle in the x–y plane with radius s and its position vector makes an angle θ with the y axis. The coordinates of atom N(2) are $(x_N, y_N, 0)$. The quinoline ring is located in the y–z plane. The nth atom in the ring has coordinates $(0, y_n, z_n)$. The distance $d_n(\theta)$ is given by

$$\begin{aligned} d_n &= \sqrt{(a_n + b_n \cos\theta)} \\ a_n &= s^2 + y_n^2 + z_n^2 \\ b_n &= -2sy_n \end{aligned} \tag{22}$$

Starting with the initial charge of the nth ring atom equal to $\rho_n(0)$, the coefficients v_l of $V(\theta)$ are[10]

$$\begin{aligned} v_0 &= \frac{e}{4\pi\varepsilon_0}\frac{1}{\sqrt{\pi}} \sum_{n=1}^{11} \rho_n(0) \sum_{m=0}^{\infty} \frac{\Gamma(2m+1/2)}{m!m!} \left(-\frac{b_n}{2}\right)^{2m} \left(\frac{1}{a_n}\right)^{2m+1/2} \\ v_{2l} &= \frac{e}{4\pi\varepsilon_0}\frac{2}{\sqrt{\pi}} \sum_{n=1}^{11} \rho_n(0) \sum_{m=l}^{\infty} \frac{\Gamma(2m+1/2)}{(m-l)!(m+l)!} \\ &\quad \times \left(-\frac{b_n}{2}\right)^{2m} \left(\frac{1}{a_n}\right)^{2m+1/2}; \quad l = 1, 2, 3, \ldots \\ v_{2l+1} &= \frac{e}{4\pi\varepsilon_0}\frac{2}{\sqrt{\pi}} \sum_{n=1}^{11} \rho(0) \sum_{m=l}^{\infty} \frac{\Gamma(2m+3/2)}{(m-l)!(m+l+1)!} \\ &\quad \times \left(-\frac{b_n}{2}\right)^{2m+1} \left(\frac{1}{a_n}\right)^{2m+3/2}; \quad l = 0, 1, 2, \ldots \end{aligned} \tag{23}$$

The θ dependence of $\rho_n(\theta)$ will be taken into account in the following fashion

$$\begin{aligned} \rho_n(\theta) &= \frac{(1+\cos\theta)}{2}\rho_n(0); \quad n = 2, \ldots, 11 \\ \sum_{n=1}^{11} \rho_n(\theta) &= -1 \end{aligned} \tag{24}$$

In this manner the negative charge will be accumulated entirely on the endocyclic N-atom ($n = 1$) at $\theta = \pi$. This is a useful feature of the model, because it implies instantaneous charge neutralization when the proton is delivered.

The initial charge distribution in the anion of 7-hydroxyquinoline has been calculated quantum chemically, using the semiempirical CNDO algorithm. Using the bond lengths, the bond angles and these calculated values of $\rho_n(0)$, the values of the coefficients v_l in eqn. (21) have been calculated. Coefficients smaller than 10^{-4} v_0 are neglected in the summation.

The required value for k_d is set equal to the value of k_d determined experimentally in the case of the reference compound 2-hydroxy-1-(*N*-morpholinomethyl)naphthalene (HMMN) *i.e.* $= k_d = 4 \times 10^8$ s^{-1}.[2] Since the rate constant for ESIPT processes within a hydrogen bond are usually larger than 10^{12} s^{-1}, the rate constant k_{PT} is assigned a value of 1×10^{12} s^{-1}.[11–13]

The basis set in eqn. (6) is truncated at $n = n_{max}$. The value of n_{max} is found by increasing its values stepwise until the numerical result from eqn. (5) does not change by more than 1 promille. The required value of n_{max} is found to increase with viscosity. In the high viscosity range, *ca.* 19 cP, its minimum value is found to be 50. This value is used throughout the whole viscosity range.

Results and Discussion

The potential $V(\theta)$ obtained after performing the summation in eqn. (21) exhibits a barrier of 88 meV at $\theta = \pm 43°$. This is shown in Fig. 2, which presents also a potential arising when the charge distribution is fixed, *i.e.* is independent of θ. In the latter case a barrier of 234 meV is obtained, nearly 10 times $k_B T$ at room temperature. An experimental value for the height of the barrier in $V(\theta)$ is obtained from the study of the isoviscous temperature dependence of k_{rot}. The experimental value, E_{act}, is 60 meV.[14] The value of E_{act} turns out to be independent of the solvent and its viscosity. The agreement between the value of E_{act} and the calculated barrier height in $V(\theta)$ indicates that the potential may be considered to be dominated by intramolecular interactions.

Fig. 3 shows the distribution function $P(\theta, t)$ for $\eta = 0.6$ cP, obtained numerically for a pinhole sink at different times, with intervals of 20 ps. The value of 0.6 cP corresponds to the viscosity of methanol at 295 K. The initial stage of the evolution of $P(\theta, t)$ is dominated by diffusion of the distribution, peaked initially around $\theta = 0$, towards large values of θ. When $P(\theta, t)$ builds up gradually at the larger values of θ, an asymmetric satellite appears just in front of the sink at $\theta = \pi$ (insert in Fig. 3). The satellite results from the θ dependence of the rate of diffusion of the Brownian particle along the trajectory. This becomes clear, when a comparison is made between particles just over the top of the barrier and those that have moved already much further in the direction of the sink. Both categories experience a force in the direction of the sink, but this force is smaller in the latter case, since the potential reaches a minimum at $\theta = \pi$ (Fig. 2). As a consequence the first category moves faster than the latter, resulting in a temporary accumulation of particles near

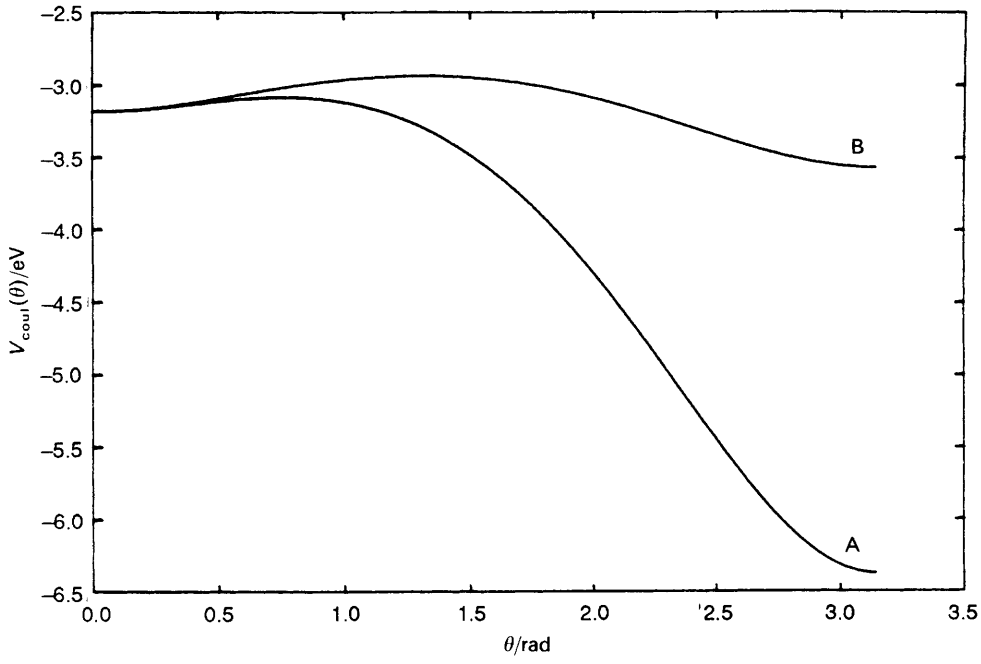

Fig. 2 Rotational potential governing the ESIPT reaction in HMMQ as calculated with the semiempirical quantum-mechanical CNDO 5 method, using a polarisable, E_{bar} = 88 meV (A) and a static, E_{bar} = 234 meV (B) charge distribution in the π-system of the chromophore

$\theta = \pi$. The asymmetry of the satellite is a consequence of the loss of the proton at the sink. In the case of a pinhole sink, the variation in $P(\theta, t)$ has been studied numerically as a function of viscosity in the range of viscosities encountered in the linear alkanols. Fig. 4 shows the result for t = 40 ps. A strong viscosity dependence can be observed in the figure. Note that the area under the curves represent the survival probability $P_e(t)$ of the population A* at time t. Fig. 5 presents the time behaviour of $P_e(t)$ in the same viscosity range. The main feature of the behaviour of $P_e(t)$ is a slow non-exponential decay at very short times ($t < 10$ ps), which changes gradually into an exponential decay at long times.

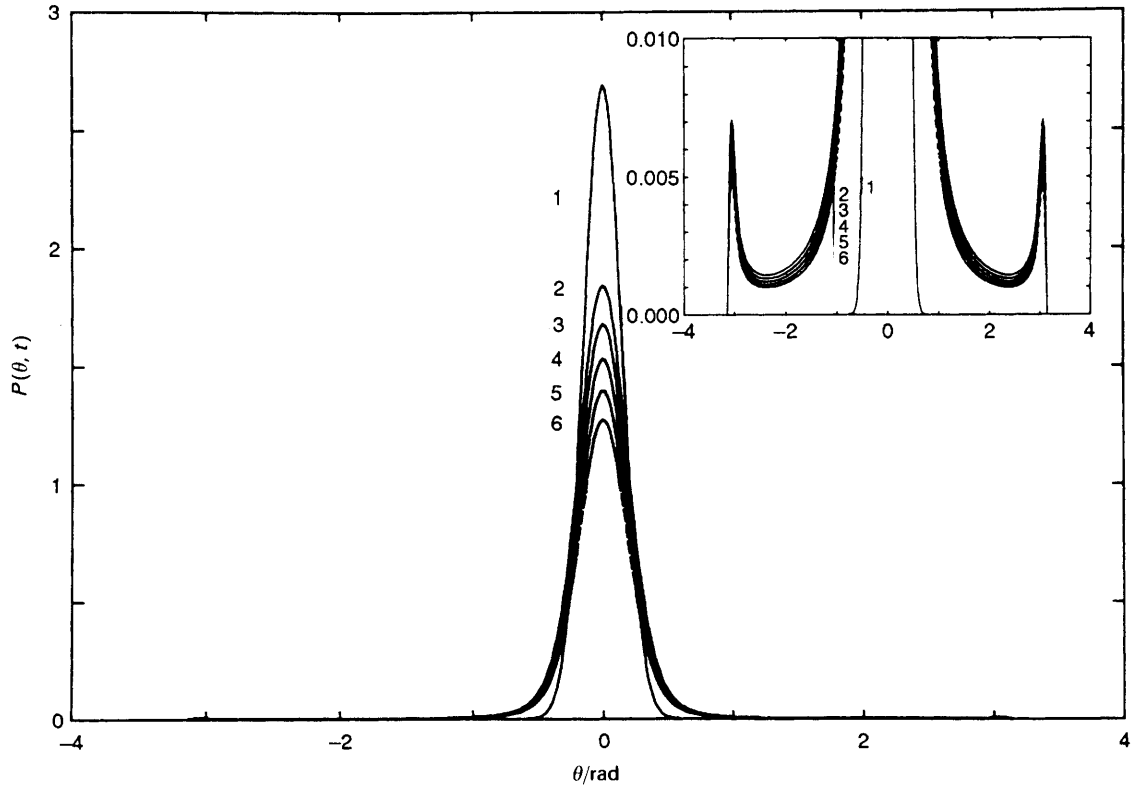

Fig. 3 Distribution function $P(\theta, t)$ at different times for a pinhole sink and a viscosity corresponding to methanol (η = 0.6 cP). t = 0 ps (1), 20 ps (2), 40 ps (3), 60 ps (4), 80 ps (5), 100 ps (6). Inset shows a close up of the region around $\theta = \pi$

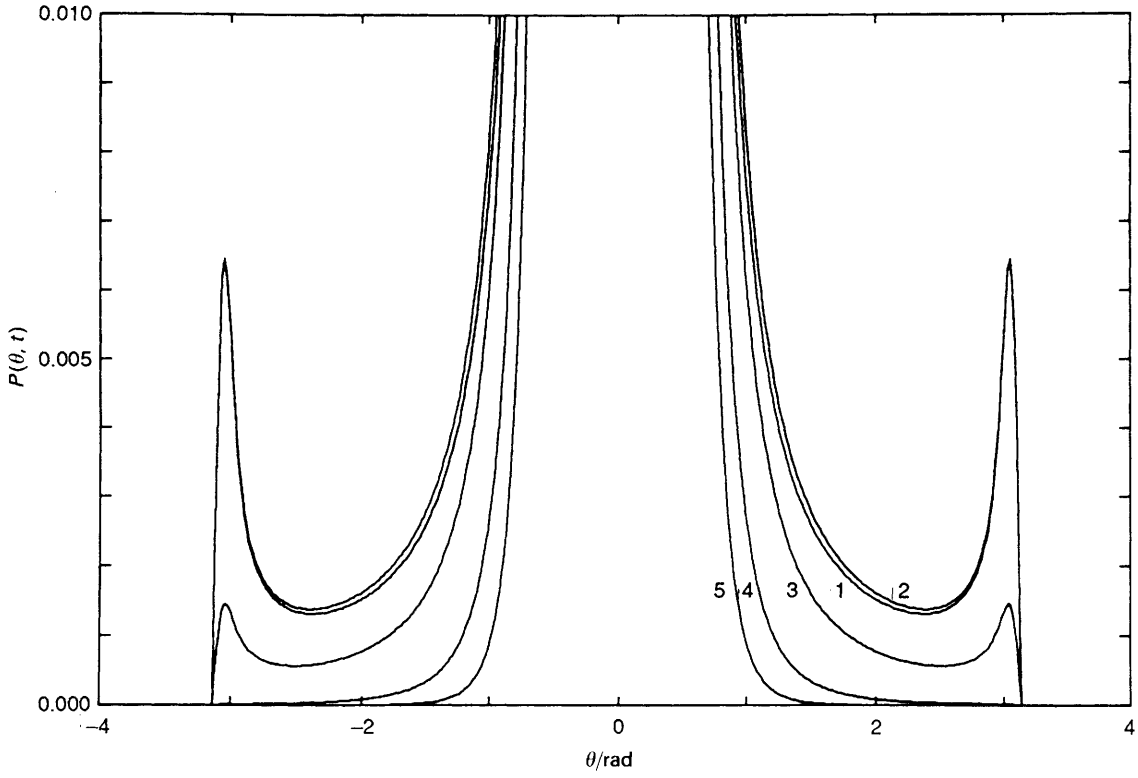

Fig. 4 Distribution function $P(\theta, t)$ at $t = 40$ ps at different viscosities, corresponding to several *n*-alkanols at room temperature: (1) methanol; (2) propan-1-ol; (3) pentan-1-ol; (4) heptan-1-ol; (5) decan-1-ol

The short-time behaviour is controlled by the diffusion of the Brownian particle along the trajectory as well as by the loss of excitation energy (k_d). In contrast the long-time behaviour is governed nearly completely by k_{PT}, because then the shape of the distribution $P(\theta, t)$ has become stationary. Then the decay constant for long times is equal to k_L given by

$$k_L \equiv \lim_{t \to \infty} \frac{\partial \ln[P_e(t)]}{\partial t} \tag{24}$$

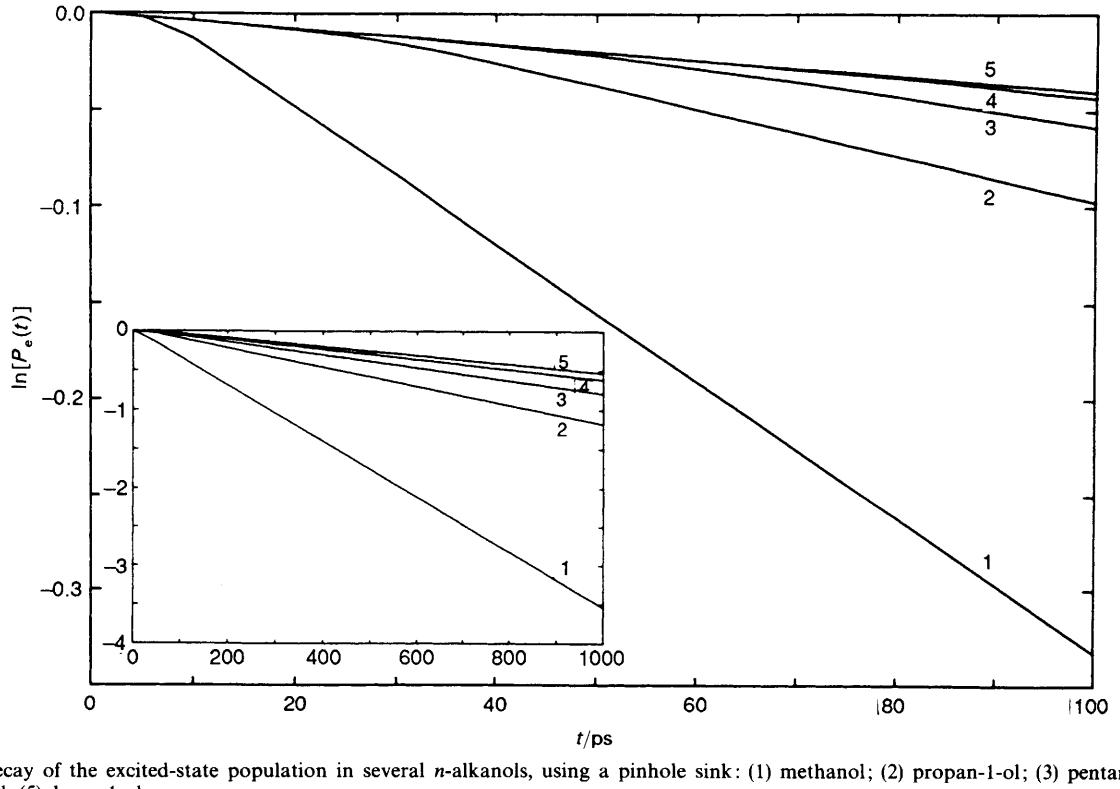

Fig. 5 Decay of the excited-state population in several *n*-alkanols, using a pinhole sink: (1) methanol; (2) propan-1-ol; (3) pentan-1-ol; (4) heptan-1-ol; (5) decan-1-ol

If the time required to reach the stationary shape of $P(\theta, t)$ is short, k_L approaches the value of k defined in eqn. (5). Since the period in which the decay of $P_e(t)$ is non-exponential is merely *ca.* 20 ps, the value of k_L is almost equal to the value of k calculated *via* eqn. (5), (16). Results similar to those obtained in the case of the pinhole sink are found when the sink is Gaussian.

In Fig. 6 and 7 the rate constant k is compared with the experimental decay rate, k_{exp}, of the population A*. Fig. 6 shows k as a function of η in the case of a series of *n*-alkanols as solvents, whereas the results for the alkanenitriles are shown in Fig. 7. Table 1 presents the values of both k and k_{exp}. The figures reveal a good agreement between the calculated and experimental values of the decay constant of the population A*. Especially at the higher viscosities the fit is very good. The calculated values are larger than the experimental ones at viscosities <1.5 cP. This may be understood by bearing in mind that the model applies strictly only in the case of overdamped motion of the side chain, *i.e.* at high viscosity, when the velocity distribution of the Brownian particle is thermally equilibrated. For low viscosities the calculated values are less accurate, since the velocity distribution does not reach equilibrium fast enough. The proper form of the operator L in the case of low viscosities is

$$L = -\dot{\theta}\frac{\partial}{\partial\theta} - \frac{F(\theta)}{I}\frac{\partial}{\partial\dot{\theta}} + \frac{\xi}{I}\left(\frac{\partial}{\partial\dot{\theta}}\dot{\theta} + \frac{kT}{I}\frac{\partial^2}{\partial\dot{\theta}^2}\right) \quad (26)$$

An interesting point to mention is that in the case of the alkanenitriles a reasonable agreement between theory and experiment, in the high viscosity range, could be achieved only by introducing in the model a Gaussian sink, $S_b(\theta)$, at $\theta = 0$, *i.e.* at the site where atom N(2) receives the proton. This sink describes the effect of a back-proton transfer to the original site, *i.e.* the O atom. The width of the Gaussian sink has been set equal to the width of $P(\theta, 0)$, *i.e.* 20° (FWHM). The rate constant, k_b, for the back transfer of the proton has been treated as an adjustable parameter in an additional term in eqn. (1), namely $-k_b S_b(\theta)P(\theta, t)$. The adjusted value of k_b is 5×10^7 s^{-1}. The absence of a back transfer in the case of alkanols must be considered to be a consequence of a hydrogen bond between the solvent and the negatively charged oxygen atom, inhibiting the return of the proton.

The calculated values of k reproduce the experimental fractional power dependence of the form $k = a\eta^{-c}$. The value of the exponent c deviates slightly from the experimental value c_{exp} in the case of the alkanols, where $c = 0.62$ and $c_{exp} =$

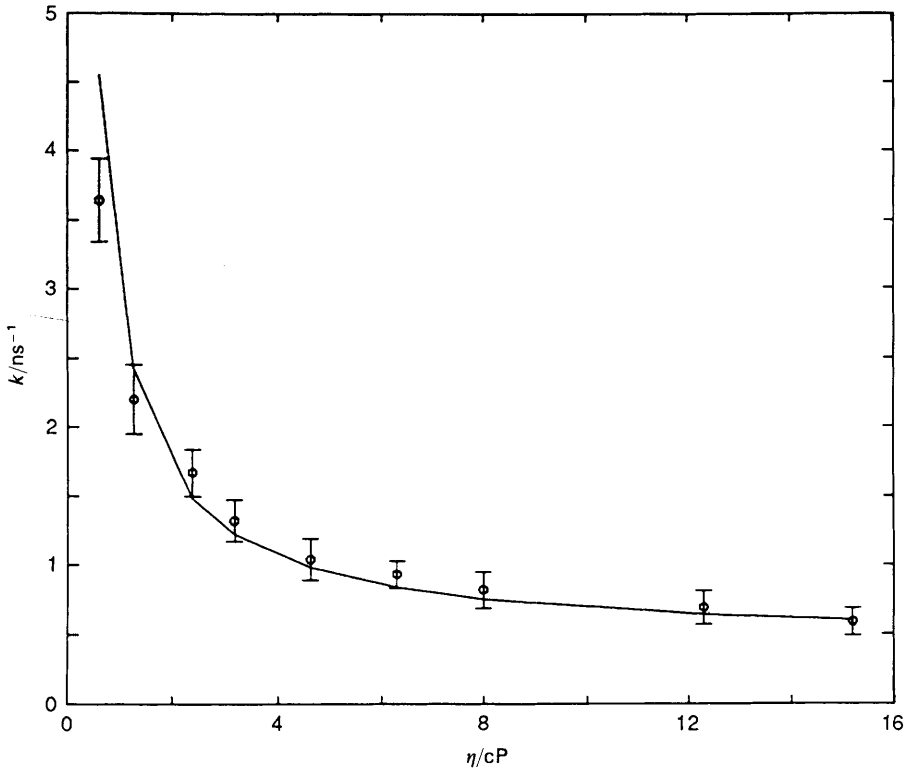

Fig. 6 Rotational rate constant as a function of viscosity for the *n*-alkanol series at room temperature. The points correspond to experimental values, while the line connects calculated points

Table 1 Experimental and calculated decay rate constants of the excited-state population of the anionic tautomer of HMMQ

solvent	η/cP	k_{exp}/ns^{-1}	k_{calc}/ns^{-1}	solvent	η/cP	k_{exp}/ns^{-1}	k_{calc}/ns^{-1}
methanol	0.61	3.64 ± 0.30	4.54	acetonitrile	0.31	3.51 ± 0.32	5.68
ethanol	1.26	2.20 ± 0.25	2.42	propiononitrile	0.45	2.99 ± 0.25	5.04
propan-1-ol	2.39	1.67 ± 0.17	1.49	butyronitrile	0.61	2.82 ± 0.22	3.95
butan-1-ol	3.18	1.32 ± 0.15	1.23	valeronitrile	0.78	2.33 ± 0.21	3.28
pentan-1-ol	4.63	1.04 ± 0.15	0.98	hexanenitrile	1.03	2.17 ± 0.20	2.70
hexan-1-ol	6.3	0.93 ± 0.10	0.83	octanenitrile	1.8	1.92 ± 0.20	1.93
heptan-1-ol	8.0	0.82 ± 0.13	0.75	nonanenitrile	2.3	1.72 ± 0.15	1.70
nonan-1-ol	12.3	0.69 ± 0.12	0.64	undecanenitrile	3.3	1.52 ± 0.11	1.46
decan-1-ol	15.2	0.59 ± 0.10	0.60				

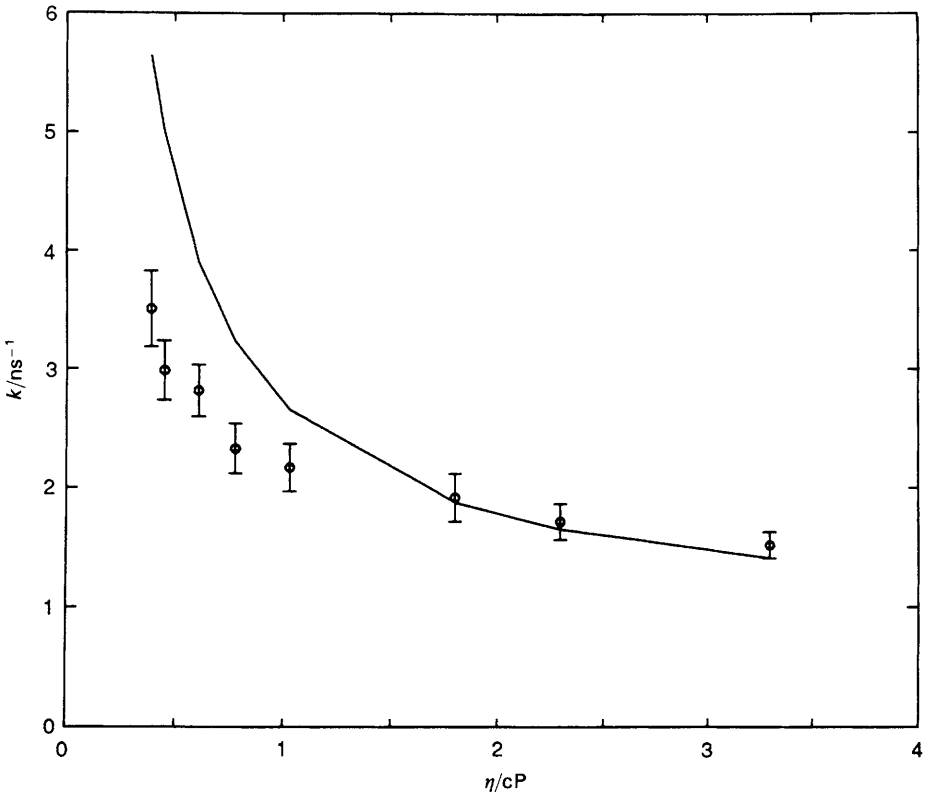

Fig. 7 Rotational rate constant as a function of viscosity for the alkanenitrile series at room temperature. The points correspond to experimental values, while the line connects calculated points

0.55. In the case of the alkanenitriles, where $c = 0.64$ and $c_{exp} = 0.37$, the deviation is large. The large deviation in the case of the nitriles must be due to fact that the viscosities of the nitriles are in the low range, where the model is imperfect. The value of c turns out to depend strongly on the competition between the position-independent deactivation on the one hand and the position-dependent proton loss on the other hand. This may be understood, by comparing the results obtained in three different cases, namely in the limit where $k_{PT} = k_b = 0$; the limit where $k_d = 0$, while the sinks are pinholes and the limit where $k_d = 0$, while the sinks are Gaussian. In the first limit, the decay of N_{A^*} does not depend on viscosity, *i.e.* $c = 0$. In the second limit, $c = 1$. In the third limit, $c < 1$ and c approaches 0, when the width of the Gaussian sinks tends to ∞. The last result arises, because of a position-independent decay of N_{A^*}, similar to the decay with rate constant k_d, whose importance increases with the width of the Gaussian sinks, resulting in a value of c intermediate between the first and second limit. In this manner, the presence of the Gaussian sink $S_b(\theta)$ is contributing to the reduction of the value of c for solutions in nitriles compared to solutions in alkanols. This effect of the relative importance of the position-independent and position-dependent sink terms on the value of c has been found previously by Bagchi *et al.* in the case of barrierless electronic relaxation.[3]

Since the proton crane carries an electrical charge, an influence of dielectric friction on its motion is to be expected. The dielectric friction may be taken into account in the equation of motion given in eqn. (2), by writing the friction coefficient for the ith solvent as a sum of a hydrodynamic and a dielectric term, each of which is proportional to η, *i.e.* as

$$\zeta(i) = \zeta_{hydr}(i) + \zeta_{diel}(i)$$
$$\zeta_{hydr}(i) = \alpha\eta(i) \qquad (27)$$
$$\zeta_{diel}(i) = \frac{\mu^2}{a^3 I}\beta_i\eta(i)$$

with α independent of solvent and β_i depending on the dielectric permittivity ε_i of the ith solvent. The quantities μ, a and I are the electric dipole moment of the solute, its cavity radius and the moment of inertia of the crane, respectively. The factor β_i is given by[15]

$$\beta_i = \frac{6(\varepsilon_i - 1)\tau_D(i)}{(2\varepsilon_i + 1)^2\eta(i)} \qquad (28)$$

where $\tau_D(i)$ is the Debye dielectric relaxation time of the ith solvent. The factor β_i becomes five times larger in going from methanol to *n*-decanol as solvent. Therefore we would not have obtained satisfactory agreement above between theory and experiment, unless ζ_{diel} were negligible compared to ζ_{hydr}. The negligible magnitude of the dielectric friction seems to disagree with the conjecture that the dielectric friction becomes smaller than the hydrodynamic friction, provided the size of the charged Brownian particle is larger than the size of the solvent molecules.[16] However, the disagreement is only apparent because our solvent molecules are effectively smaller than their physical size. This is due to the flexibility of their alkyl chains, which enables the Brownian particle to move through the solvent by displacing only small segments of the solvent molecules.

Note that the fractional power dependence of k on η is obtained here by disregarding any time dependence in the friction coefficient ξ. Such a time dependence in ξ has been shown to be important, when the rate of fluctuations in the random force is comparable to the rate of barrier crossing.[16] In a forthcoming paper, experimental results on photoinduced proton transfer in derivatives of HMMQ will be presented, which cannot be understood within the present model, but which may be explained with the Grote and Hynes model, incorporating a time-dependent ξ.

This work was supported by the Foundation for Chemical Research in the Netherlands (S.O.N.) with financial aid from the Netherlands Organization for the Advancement for Pure

Research (N.W.O.). The authors wish to thank Dr. G. van der Zwan for enlightening discussions.

References

1 C. J. Jalink, A. H. Huizer and C. A. G. O. Varma, *J. Chem. Soc., Faraday Trans. 2*, 1990, **86**, 3712.
2 C. J. Jalink, W. M. van Ingen, A. H. Huizer and C. A. G. O. Varma, *J. Chem. Soc., Faraday Trans.*, 1991, **87**, 1103.
3 B. Bagchi, G. R. Fleming and D. W. Oxtoby, *J. Chem. Phys.*, 1983, **78**, 7375.
4 S. Chandrasekhar, *Rev. Mod. Phys.*, 1943, **15**, 1.
5 N. G. van Kampen, *Stochastic Processes in Physics and Chemistry*, North-Holland, Amsterdam, 1981.
6 H. Risken, *The Fokker–Planck Equation*, Springer-Verlag, Berlin, 1984.
7 B. Bagchi and G. R. Fleming, *J. Phys. Chem.*, 1990, **94**, 9.
8 H. Sumi and R. A. Marcus, *J. Chem. Phys.*, 1986, **84**, 4894.
9 W. Nadler and R. A. Marcus, *J. Chem. Phys.*, 1987, **86**, 3906.
10 I. S. Gradshteyn and I. M. Ryzhik, *Table of Integrals, Series and Product*, Academic Press, San Diego, 1980, p. 374.
11 C. J. Jalink, A. H. Huizer and C. A. G. O. Varma, Proc. U.P.S. '91, 7–11 October 1991, Bayreuth, Germany; *J. Chem. Soc., Faraday Trans.*, to be submitted.
12 J. Konijnenberg, A. H. Huizer and C. A. G. O. Varma, *J. Chem. Soc., Faraday Trans. 2*, 1988, **84**, 363.
13 J. Konijnenberg, A. H. Huizer and C. A. G. O. Varma, *J. Chem. Soc., Faraday Trans. 2*, 1988, **84**, 1163.
14 J. Konijnenberg, A. H. Huizer and C. A. G. O. Varma, *J. Chem. Soc., Faraday Trans. 2*, 1989, **85**, 1539.
15 B. Bagchi, *J. Chem. Phys.*, 1991, **95**, 467.
16 R. F. Grote and J. T. Hynes, *J. Chem. Phys.*, 1980, **73**, 2715.

Paper 2/01059C; *Received* 28*th February*, 1992